ESAS-Derived Earth Departure Stage Design for Human Mars Exploration

Kevin Flaherty, Michael Grant, Ashley Korzun, Faure Malo-Molina,
Bradley Steinfeldt, Benjamin Stahl, Alan Wilhite
Georgia Institute of Technology, Atlanta, GA 30332-0150

Table of Contents

ESAS-Derived Earth Departure Stage Design for Human Mars Exploration 1
Nomenclature 2
I. Introduction 2
Background 2
Motivation 3
Scope 3
Elements of the Earth Departure Stage 3
II. Systems Engineering Process 4
Process Planning 4
Figures of Merit 4
Analytic Hierarchy Process 4
Technique for Ordered Preference by Similarity to Ideal Solution 5
Design Convergence 5
Requirements Analysis 6
Trade Space 6
III. Methodology 7
Ascent Trajectory Analysis 7
Transfer Trajectory Analysis 10
Sizing 13
Propulsion System 13
Other Subsystems 14
Payload Division 15
Propellant Depot 15
Cost Analysis 15
Reliability Analysis 16
IV. Results 16
Earth Departure Stage Solutions 16
Design Space 16
Factor Contribution to Results 18
Selected Design 18
Vehicle Definition 18
Mass Breakdown 19
Configuration 19
V. Risk Assessment and Mitigation 20
Risk Assessment 20
Technology Impact 21
VI. Conclusions and Further Study 21
References 22

ESAS-Derived Earth Departure Stage Design for Human Mars Exploration

Kevin Flaherty*, Michael Grant*, Ashley Korzun*, Faure Malo-Molina*,
Bradley Steinfeldt*, Benjamin Stahl*, Alan Wilhite†
Georgia Institute of Technology, Atlanta, GA 30332-0150

The Vision for Space Exploration has set the nation on a course to have humans on Mars as early as 2030. To reduce the cost and risk associated with human Mars exploration, NASA is planning for the Mars architecture to leverage the lunar architecture as fully as possible. This study takes the defined launch vehicles and system capabilities from ESAS and extends their application to DRM 3.0 to design an Earth Departure Stage suitable for the cargo and crew missions to Mars. The impact of a propellant depot in LEO was assessed and sized for use with the EDS.

To quantitatively assess and compare the effectiveness of alternative designs, an initial baseline architecture was defined using the ESAS launch vehicles and DRM 3.0. The baseline architecture uses three NTR engines, LH2 propellant, no propellant depot in LEO, and launches on the Ares I and Ares V. The Mars transfer and surface elements from DRM 3.0 were considered to be fixed payloads in the design of the EDS.

Feasible architecture alternatives were identified from previous architecture studies and anticipated capabilities and compiled in a morphological matrix. ESAS FOMs were used to determine the most critical design attributes for the effectiveness of the EDS. The ESAS-derived FOMs used in this study to assess alternative designs are effectiveness and performance, affordability, reliability, and risk. The individual FOMs were prioritized using the AHP, a method for pairwise comparison. All trades performed were evaluated with respect to the weighted FOMs, creating a Pareto frontier of equivalently ideal solutions. Additionally, each design on the frontier was evaluated based on its fulfillment of the weighted FOMs using TOPSIS, a quantitative method for ordinal ranking of the alternatives.

The designs were assessed in an integrated environment using physics-based models for subsystem analysis where possible. However, for certain attributes such as engine type, historical, performance-based mass estimating relations were more easily employed. The elements from the design process were integrated into a single loop, allowing for rapid iteration of subsystem analyses and compilation of resulting designs.

Several key trades were performed to improve the baseline architecture. The principle design driver for the EDS is the selection of a propulsion system. Primary propulsion options include nuclear-thermal and chemical systems as well as multiple propellant types. Another important consideration is the flexibility of a

* Graduate Research Assistant, Guggenheim School of Aerospace Engineering
† NASA Langley Professor in Advanced Aerospace Systems Architecture, Guggenheim School of Aerospace Engineering

multi-launch mission, which affects the probability of success of the mission and includes the option of using a propellant depot in LEO to increase launch flexibility. Using a propellant depot in LEO also allows the fill regimen for the boosted EDS to be traded. This study provides an optimized EDS design, improving on the DRM baseline by 15% in cost and 19% in reliability.

Nomenclature

ADCS	=	Attitude Determination and Control
AHP	=	Analytic Hierarchy Process
C&DH	=	Command and Data Handling
CEV	=	Crew Exploration Vehicle
DRM	=	Design Reference Mission
DSM	=	Design Structure Matrix
EDS	=	Earth Departure Stage
ESAS	=	Exploration Systems Architecture Study
FOM	=	Figure of Merit
GA	=	Genetic Algorithm
IMLEO	=	Initial Mass in Low Earth Orbit
LEO	=	Low Earth Orbit
LOM	=	Loss of Crew
LOV	=	Loss of Vehicle
MDS	=	Mars Departure Stage
MECO	=	Main Engine Cutoff
MER	=	Mass Estimating Relationship
NAFCOM	=	NASA/Air Force Cost Model
NTR	=	Nuclear Thermal Rocket
OEM	=	Overall Evaluation Metric
POST	=	Program to Optimize Simulated Trajectories
PSO	=	Particle Swarm Optimizer
RSE	=	Response Surface Equation
SBC	=	JAQAR Swingby Calculator
SOI	=	Sphere of Influence
TLI	=	Trans-Lunar Injection
TMI	=	Trans-Mars Injection
TOF	=	Time of Flight
TOPSIS	=	Technique for Ordered Preference by Similarity to Ideal Solution
$C3$	=	Specific Orbit Energy Squared
h	=	Altitude
h_d	=	Desired MECO Altitude
h_f	=	Actual MECO Altitude
m_p	=	EDS Propellant Mass
V	=	Velocity
V_d	=	Desired MECO Velocity
V_f	=	Actual MECO Velocity
ΔV	=	Velocity Change
α	=	MECO Target Penalty Coefficient
β	=	MECO Propellant Penalty Coefficient
γ	=	Flight Path Angle
γ_d	=	Desired MECO Flight Path Angle
γ_f	=	Actual MECO Flight Path Angle
ψ	=	Mass Penalty Coefficient

I. Introduction

Background

The Vision for Space Exploration mandated the goal of returning humans to the Moon by 2020 and sending a manned mission to Mars as early as 2030. In response, NASA commissioned the Exploration Systems Architecture Study (ESAS), presenting a full lunar architecture and a proposed Mars design reference mission. The proposed reference mission describes a 1000-day mission with a 500-day stay on the Martian surface. Surface infrastructure is emplaced two years prior to the human landing. While lunar exploration elements are leveraged to decrease cost and risk, this study outlines the systems and technologies required to enable a human mission, including propulsion systems, tank materials, and a propellant depot in LEO. The key elements of the ESAS architecture are the Ares I and Ares V launch vehicles to boost elements into LEO, the EDS, the CEV, the Mars ascent vehicle, and the MDS. Figure 1 shows the ESAS Mars DRM.

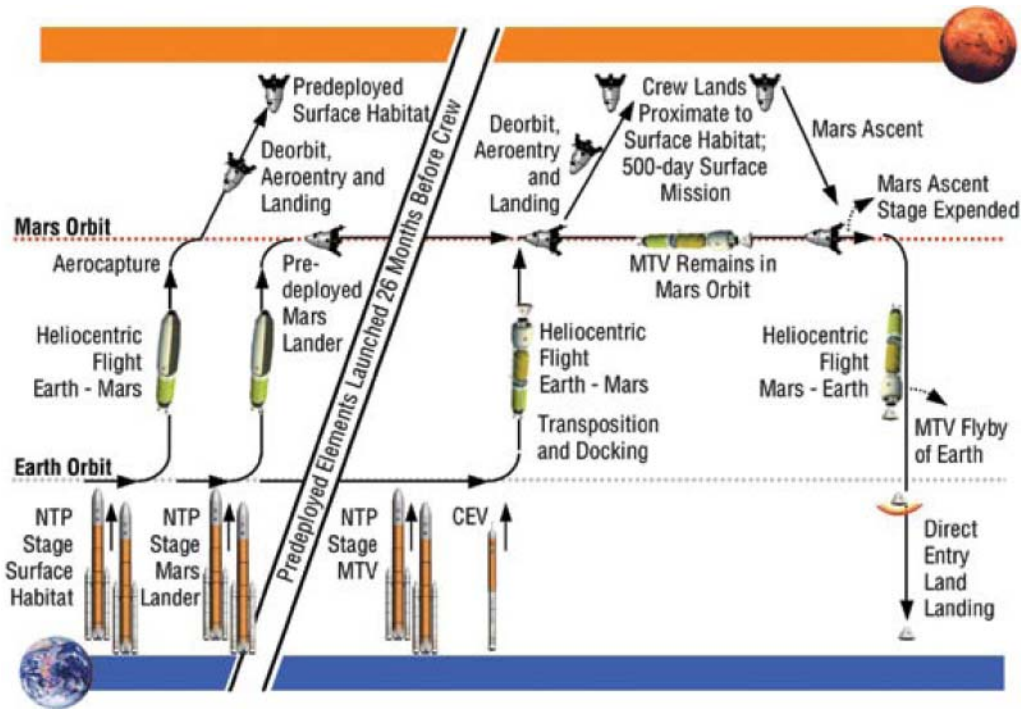

Figure 1. ESAS Design Reference Mission for Mars Exploration[1].

Motivation

The definition of architectures to explore Mars through science missions, robotic precursors, and an eventual human presence will evolve into a focal point for NASA as the lunar program moves forward and the space shuttle is retired. These infrastructure concepts and aggressive objectives require landed masses an order of magnitude or greater than any Mars mission previously planned or flown. This study details an EDS concept to deliver crew, cargo, and the supporting infrastructure to Mars. The technology development necessary to undertake this task was analyzed, and alternative concepts were traded to converge on a cost effective, risk-averse solution. To be consistent with current exploration goals, the concept uses elements of ESAS and DRM to expand the design space and evolve a more optimal design for the EDS. The results of this study detail alternative EDS designs in support of the human exploration of Mars, along with supporting analyses and rationale.

Scope

The scope of this study was to develop and assess alternative concepts for an EDS for human Mars missions based on requirements from ESAS and DRM. The design focuses on the launch, ascent, and interplanetary transfer phases of the mission in defining the EDS. Only Ares I and Ares V launch vehicles were considered, with the performance of the Ares V first stage fixed. Payload masses for the EDS were fixed directly from DRM 3.0. The vehicle design was developed independently from the MDS, which will return the crew to Earth after the Mars surface stay. The arrival at Mars was excluded from the analysis.

The trade space for the EDS was expanded beyond subsystem components to allow for alternative elements including a propellant depot in LEO and an alternate Ares V upper stage. The intent of this study was to provide a design alternative which allows for an assessment of the current state of the art and the necessary provisions that must be enacted to pursue human Mars missions.

Elements of the Earth Departure Stage

The EDS configuration developed and selected in this study is a nearly self-sufficient spacecraft with subsystems supplying power, propulsion, thermal control, attitude determination and control (ADCS), propellant storage, and an unpressurized structure in support of the payloads to be delivered from LEO to Mars. Both power and propulsion are provided by a bi-modal NTR, where reactor heat is converted to usable power using a Brayton cycle engine and regulated for use by the EDS and payload. Propellant is

stored as liquid hydrogen and is heated directly by the reactor to accelerate the propellant through two nozzles. Channeling and radiating excess reactor heat actively provides thermal control. Attitude control is achieved using small hydrazine thrusters.

II. Systems Engineering Process

Process Planning

Figures of Merit

ESAS defines five figures of merit (FOMs) for the assessment of alternative concepts: safety and mission success, effectiveness and performance, extensibility and flexibility, programmatic risk, and affordability. In this study, ESAS-derived FOMs for effectiveness and performance, affordability, and reliability were used to compare alternative concepts and ultimately select the best overall design for a Mars mission EDS. Figure 2 shows a breakdown of the criteria each concept was quantitatively or qualitatively assessed against.

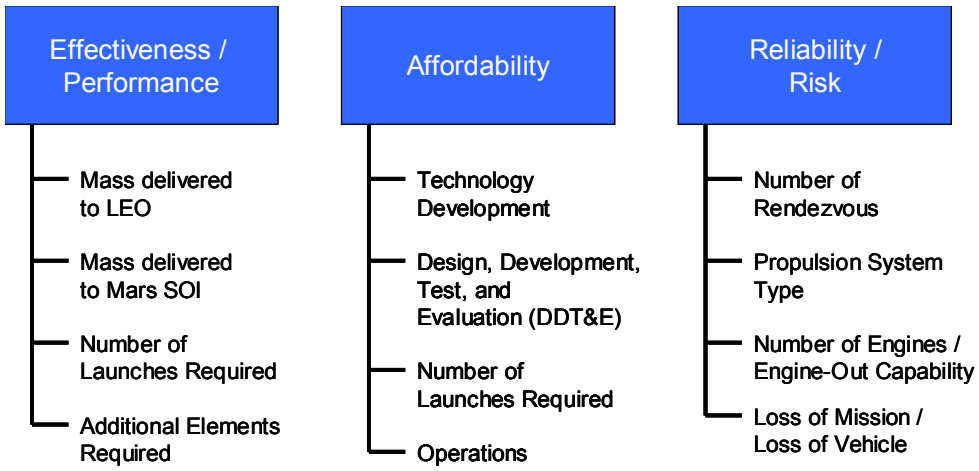

Figure 2. Figures of Merit.

Analytic Hierarchy Process

The overall objective in this design process was to create a multi-dimensional surface of the best alternatives for the EDS configuration in terms of the various FOMs, with the selection of a design on the Pareto frontier requiring the determination of a relative prioritization vector. The Analytic Hierarchy Process (AHP) is a multi-attribute decision making methodology developed by Dr. Thomas Saaty[5] for creating this priority vector. AHP assumes that problems can be decomposed into a hierarchy of decision criterion which are compared to one another using pairwise comparison. These pairwise comparisons form a decision matrix. After normalization, the average value in each row forms the prioritization vector for each respective FOM. AHP can also be extended to selection of alternatives, although it becomes time intensive to form the matrix of pairwise comparisons with a large number of alternatives.

As discussed above, the ESAS FOMs were reduced into three easily quantifiable parameters: reliability, performance, and affordability. However, all designs were required to meet the same performance floor. Accordingly, for comparison purposes, the FOMs of interest were reliability and affordability. For these two FOMs, the normalized pairwise comparison matrix obtained through AHP is shown in Table 1, along with the priority vector used to downselect among the alternative EDS designs. To identify the best alternative, reliability was weighted two times greater than affordability.

Table 1. Normalized Pairwise Comparison Matrix.

	Reliability/Risk	*Affordability*	*Priority*
Reliability/Risk	0.67	0.67	*0.67*
Affordability	0.33	0.33	*0.33*

According to Table 1, for purposes of identifying the best alternative, safety and mission success is weighted two times greater than affordability.

Technique for Ordered Preference by Similarity to Ideal Solution

Due to the time-intensive nature of AHP as the number of alternatives increases, the Technique for Ordered Preference by Similarity to Ideal Solution (TOPSIS) was implemented to select the best overall EDS design using the prioritization vector determined from AHP. In TOPSIS, the best alternative design is found by identifying the alternative with the maximum Euclidean distance from the negative ideal solution and the minimum Euclidean distance from the positive ideal solution. The closeness is determined from these two Euclidean distances, and the alternative with closeness nearest to unity is the preferred alternative design.

Design Convergence

In the initial phase of this study, an iterative design process was defined that uses the payload and mission objectives to design and optimize an EDS architecture. Figure 3 shows a DSM representation of the design process with information feed-forward in the top-right and feedback in the bottom-left. The feed-forward mirrors the interactions of analysis tools used to calculate system parameters. The feedback was eliminated by performing a full-factorial analysis of the design space to find the optimal configuration, eliminating the need for an optimization algorithm

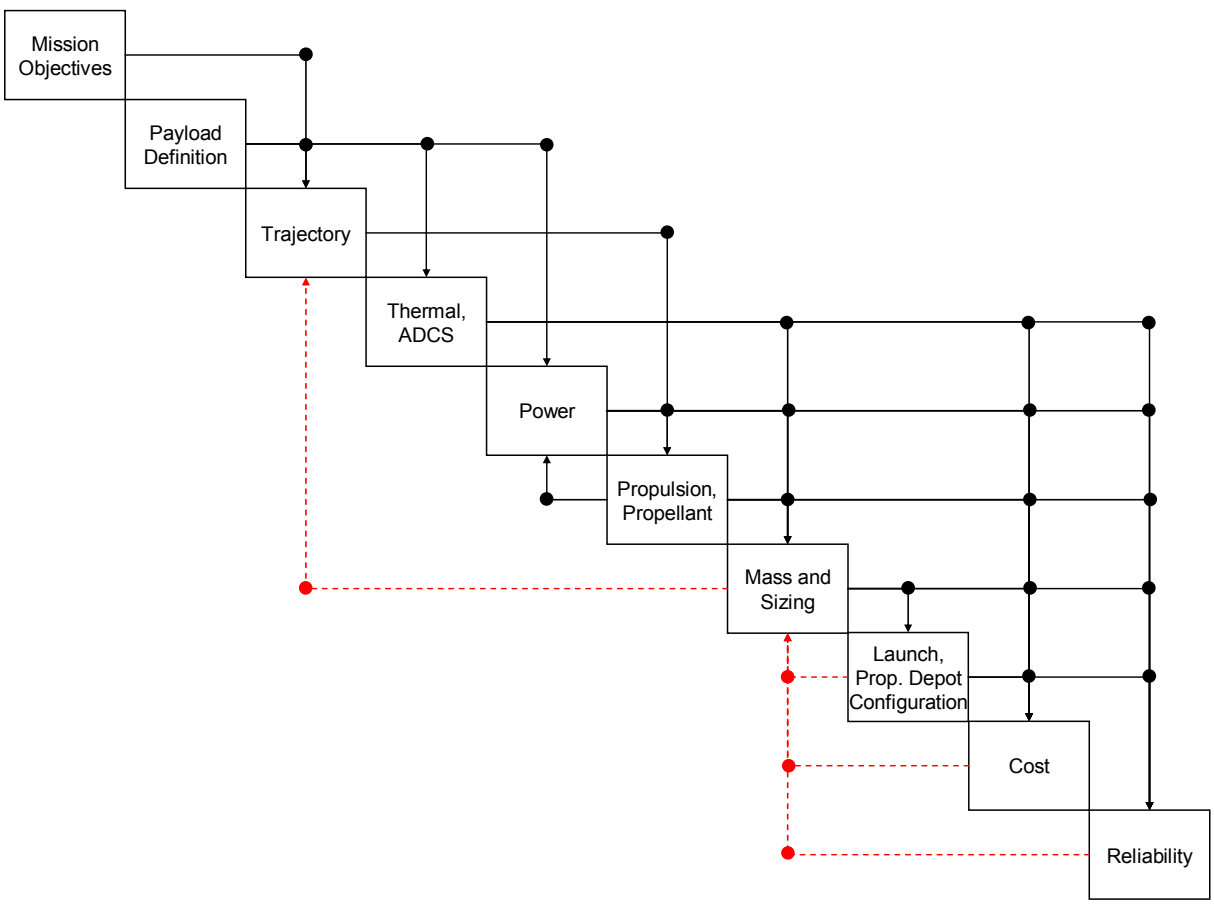

Figure 3. DSM for an Iterative Design Process.

Requirements Analysis

As discussed in Section I, the scope of this study was to define an EDS for a Mars mission by extending the capabilities of ESAS to satisfy the mission objectives outlined in DRM 3.0. Level 0 and Level 1 requirements were developed to ensure the final EDS design was compatible with the EDS requirements in both DRM 3.0 and the ESAS Mars DRM. Additionally, these requirements allowed for a direct comparison of the EDS presented in this study with the EDS in ESAS and DRM. Level 0 and Level 1 requirements are given in Table 2.

Table 2. Level 0 and Level 1 Requirements.

	Requirement ID	*Description*
Level 0	L0.1	The departure stages shall support the payload masses as provided by DRM 3.0 and ESAS
	L0.2	The departure stage shall be sized for the manned mission transit with appropriate deviations for cargo missions
	L0.3	The architecture shall adhere to all NASA standards and safety documentation as defined by ESAS
	L0.4	Ground Rules and Assumptions defined in ESAS Section 1.2 shall be followed
Level 1	L1.1	The maximum cargo transit time shall be 600 days
	L1.2	The system shall be capable of transfer during each synodic period opportunity
	L1.3	Rendezvous between cargo elements and the Earth departure stage shall occur in a 160 km circular orbit in LEO
	L1.4	The departure stage shall be capable of transferring a maximum of 75 t to Mars orbit
	L1.5	All technologies shall have be at least TRL 6 by Phase B
	L1.6	The system shall have not have a loss of mission in fewer than 250 flights
	L1.7	The system shall leverage components from the Earth departure stage for Mars departure stage

Trade Space

After defining the scope of this study and the associated requirements on the design, the trade space was created from a morphological matrix, or matrix of the alternative concepts to be analyzed. The baseline concept was taken to be the DRM 3.0 EDS, denoted in Table 3 by the highlighted alternatives.

Table 3. Matrix of Alternatives.

Attributes	*Option 1*	*Option 2*	*Option 3*	*Option 4*
Mission Duration				
Outbound Cargo	Short	**Medium**	Long	
Technology				
Tank Components	Material	**Insulation**	Cryocooler	
Structure	Composite	**Alloys**		
Propulsion Type	**NTR**	Chemical	Electric	
Propellant Type	**LH2**	LOX/CH4	LOX/LH2	Other
Propellant Depot Usage	**Never**	LEO		
EDS Configuration				
Resizing	**Cargo/Crew Independent**	Cargo/Crew Dependent		
Fill Regimen	Launch with Max Payload (Displace Prop)	**ESAS Fill**	Launch with Full Fill (Displace Cargo)	
Staging for Transfer	**Single**	Multistage		
Payload Manifesting	**DRM 3.0**	Optimal Split		
Engine Out Capability				
Trans Mars Injection	**No**	Yes		
TMI Element	**ESAS EDS**	Modified EDS	New	

The most critical attributes were determined using AHP to weight each of the ESAS FOMs and assess the relative contributions of each attribute listed in the leftmost column of Table 3. Propulsion system type, propellant choice, usage of a propellant depot in LEO, fill regimen, and launch manifesting of the required payloads were the dominant attributes in the priority vector. These attributes are shown in red in Table 3.

III. Methodology

Ascent Trajectory Analysis

Motivation

Multiple launches on the Ares V will be required for a human mission to Mars. It is likely that the payload masses of each launch will differ from those necessary for lunar exploration. In ESAS, the upper stage is used to deliver payload to orbit while containing a significant amount of residual propellant to perform the Trans-Lunar Injection (TLI) burn. However, for a Mars architecture, the upper stage is only used to deliver large payloads to LEO. Consequently, the upper stage will have to be redesigned with smaller tanks, effectively substituting the TLI propellant used in ESAS for payload to LEO for a Mars mission. The sizing of the upper stage, in conjunction with trajectory design, allows for optimal solutions to deliver heavy payloads to the desired Main Engine Cutoff (MECO) conditions.

Optimization

The optimization process was designed to determine the minimum upper stage propellant mass and open-loop thrust angle profile of the Ares V first and second stages necessary to deliver a given payload to the desired MECO conditions. These conditions correspond to the optimal MECO targets to place the vehicle into a 30x160 nm orbit at 28.5^{o} inclination and are shown in Table 4, along with the tolerances used in the optimization process detailed below[1]. The vehicle then performs a circularization burn at 160 nm altitude. The ascent trajectories were simulated using Program to Optimize Simulated Trajectories (POST).

Historically, the upper stage propellant mass was guessed, and the stage was sized using an Ares V weights and sizing model based on historical mass estimating relationships[6]. The corresponding masses of the entire stack were then transferred into POST. An optimizer would then be used to determine the optimal thrust angle profile, subject to the desired final conditions. The resulting upper stage propellant burned would be entered into the sizing tool, the Ares V would be resized, and the values would be returned to POST. This iterative process would continue until the guessed upper stage propellant mass equaled the propellant mass consumed by the optimal POST trajectory. To provide the capability to rapidly perform ascent trajectory and upper stage sizing optimization for various payloads, a MATLAB environment was created to link the sizing to various optimizers. The POST optimizers are local optimization algorithms. To explore whether these local searching algorithms identify the optimal solutions, global optimization algorithms, a genetic algorithm (GA) and particle swarm optimization (PSO), were implemented.

Table 4: MECO Targets.

Target Values	γ (deg)	h (ft)	v (ft/s)
Desired	1.0155637	473329	25707
Tolerance	2	2000	1000

Both the GA and PSO have been shown to be effective optimization algorithms. The GA is based on the evolutionary concept of the "survival of the fittest" in which the design space characteristics of good solutions have a higher chance of being retained from generation to generation during the search for the global optimum. The PSO is based on swarming theory[7]. The major advantage of PSO is the communication among particles in the population during the search of the design space for global optimal solutions. The PSO has proven to be an effective, automated means to perform global optimization of POST entry trajectories for the Mars Science Laboratory[8]. During optimization using the GA and PSO, the POST optimizer was deactivated, and POST was only used to simulate the trajectory defined by the conditions provided by the GA and PSO. To reach the desired MECO targets, penalty functions were implemented, since most of the design space results in solutions that do not meet the MECO targets. The cost function for the external optimizers is shown in Equation 1 where m_p is the EDS propellant mass, γ_f is the MECO flight path angle, γ_d is the desired MECO flight path angle, γ_{tol} is the MECO flight path angle tolerance, h_f is the MECO altitude, h_d is the desired MECO altitude, h_{tol} is the MECO altitude tolerance, V_f is the MECO velocity, V_d is the desired MECO velocity, V_{tol} is the MECO velocity tolerance, and α is the MECO penalty coefficient, β is the penalty associated when more propellant was consumed than provided, $m_{p,used}$ is the propellant mass consumed by the upper stage calculated in POST, and Ψ is the ground impact penalty.

The overall goal was to minimize the propellant mass necessary to reach the MECO targets. The coefficient values were largely determined by the user, but take various values, depending on the optimization algorithm used. The constant value of α was determined by the user and is the artificial increase in upper stage propellant when the MECO flight path angle, altitude, and velocity deviate from the desired values by the corresponding tolerances.

During the ascent trajectory, POST computes a mass flow rate corresponding to the thrust provided by the upper stage engine. POST does not track the amount of propellant mass contained in the EDS. Thus, the mass of the vehicle is simply decreased throughout ascent, resulting in the eventual consumption of inert mass. Hence, the penalty β was used to substantially penalize the solution if POST used more propellant mass than allotted by the optimizer. The final constant penalty ψ was used to dramatically penalize solutions that impact the ground, ensuring such regions are found to be undesirable by the optimizer. As expected, the posed optimization was challenging, requiring many penalty functions, with the parameters for these penalty functions specified in Table 5. Comparing the performance of the GA and PSO, the PSO consistently identified better solutions than the GA, eliminating the GA as a viable analysis option.

$$J = m_p + \alpha\left(\frac{\left|\gamma_f - \gamma_d\right|}{\gamma_{tol}} + \frac{\left|h_f - h_d\right|}{h_{tol}} + \frac{\left|V_f - V_d\right|}{V_{tol}}\right) + \beta\left(m_{p,used} - m_p\right) + \psi \tag{1}$$

Table 5: Penalty Parameters.

Algorithm	*α*	*β*	*ψ*
GA	10000	1.00E+06	1.00E+12
PSO	50000	1.00E+10	1.00E+18

To optimize the size of the Ares V upper stage to deliver a given payload to orbit, a Pareto front was generated using the POST optimizer. The optimizing script swept through payload masses ranging from 200 to 400 kip (90.7 MT to 181.4 MT) in 1 kip increments, to span the range of possible EDS payload sizes.

During the sweep, the core stage dry weight, upper stage dry weight, and total vehicle initial weight were all calculated using the MATLAB Ares V weights and sizing tool mentioned above. In this process, the first stage of the Ares V was not resized; only the upper stage fluctuated to accommodate the varying payloads. This allowed the proposed design to utilize the Ares V first stage without modification and the optimized upper stage to deliver the payload to orbit. The inputs to the weights and sizing tool are the desired LEO payload and the upper stage propellant mass. Because the optimizer is calculating the upper stage propellant mass, this value was estimated up front in order to size the rest of the vehicle. The guess corresponded to the converged upper stage propellant mass from the previous iteration, ensuring that the value was near to the actual value of the upper stage propellant mass. The script then generated a POST input deck with the weights calculated by the weights and sizing tool. The input deck was run through the POST optimizer, and the actual total vehicle initial weight, upper stage dry weight, upper stage propellant mass, and MECO condition errors were all stored.

A comparison was performed between the Pareto fronts, relating payload mass in LEO to the Ares V upper stage propellant mass, generated by POST and PSO. These fronts appear in Figure 4. As shown, the POST optimized solutions are better than those solutions obtained by the PSO for most payload masses. A plot of the MECO altitude and flight path errors for both algorithms is plotted versus payload in Figure 5. The PSO algorithm was not capable of reaching the MECO targets with high precision and was likely a major consequence of the use of penalty functions. Thus, for low payload masses, POST was able to obtain solutions with less upper stage propellant mass while reaching the MECO targets with better precision. For the large payload of 360 kip (163.3 MT), the swarm solution yielded an improved propellant mass while reaching the MECO targets with less error. This was likely due to the difficulty of actually delivering such heavy payloads to LEO when the first stage of the Ares V is fixed. Additionally, the computation time required for each PSO solution was orders of magnitude larger than that required by POST, demonstrating the capability of POST to find globally optimal solutions with minimal computational time.

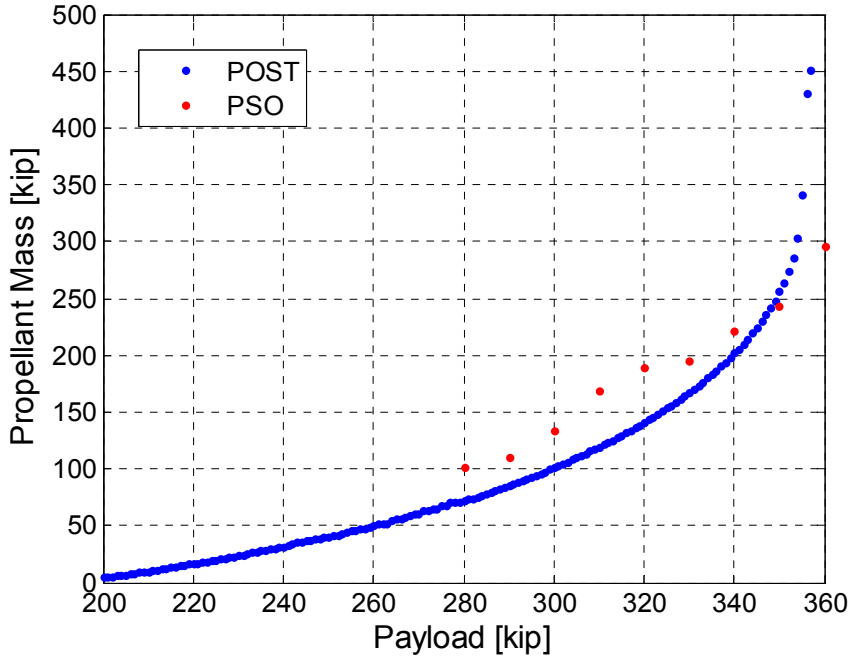

Figure 4. Pareto Front of Upper Stage Propellant Mass and Payload.

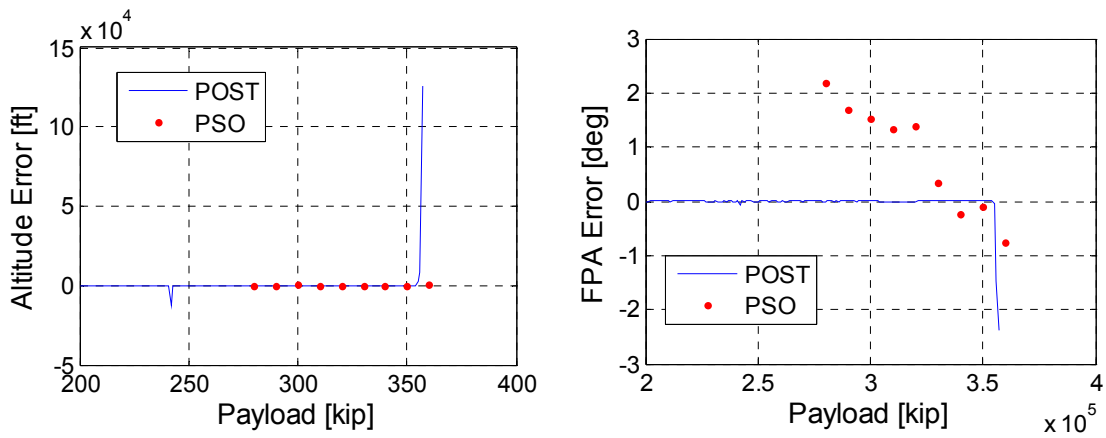

Figure 5. Altitude and FPA Error vs. Payload.

The optimal trajectories corresponding to various points throughout the Pareto front are shown in Figure 6. The lighter payloads yielded optimal trajectories that quickly gained altitude and were able to meet the MECO conditions relatively close to the launch site. However, as the payload mass increased, the vehicle had to travel farther downrange to acquire orbital velocity at the required altitude. As the payload was increased to the limits of the capability of the vehicle, lofted trajectories were flown in which the vehicle drooped in altitude while accelerating to orbital velocity.

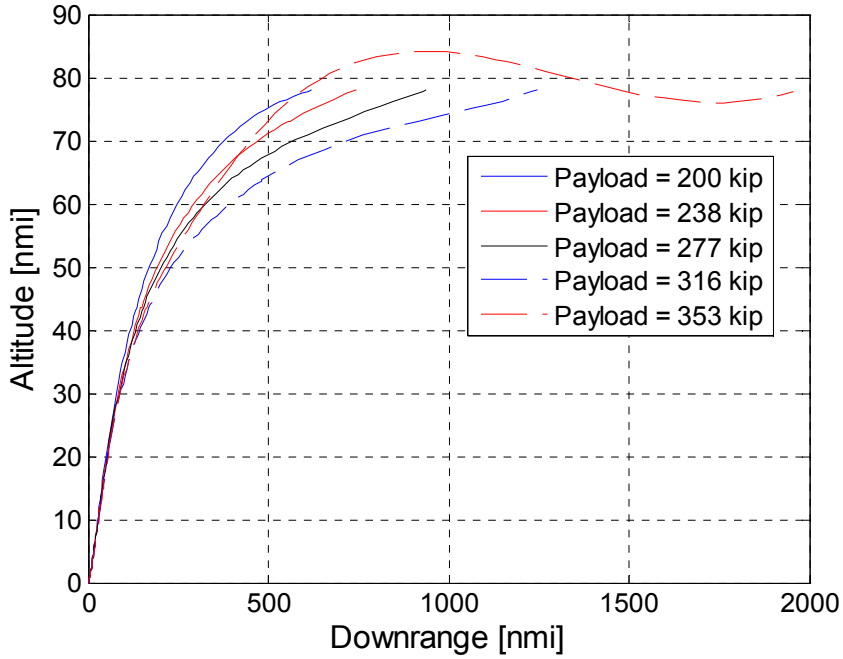

Figure 6. Optimal Trajectories for Various Payload Masses.

The ESAS-defined Ares V delivers 366 kip (166 MT) of payload to LEO, which includes 271 kip (123 MT) of upper stage TLI propellant. This corresponds to an upper stage ascent propellant mass of 224 kip (101.6 MT). For missions utilizing an NTR for the TMI maneuver, additional upper stage propellant is not beneficial. The nominal payload mass that must be delivered to LEO by the upper stage for a human Mars mission is 290 kip (131.5 MT). This payload mass corresponds to an upper stage propellant mass of only 86 kip (39 MT), as shown in Figure 4. Consequently, the upper stage tank mass and volume can be drastically reduced for the nominal Mars mission. This increases the efficiency of the upper stage to deliver the required payload to LEO. This also accommodates the larger volume payloads necessary for Mars missions.

Transfer Trajectory Analysis

Once in LEO, the EDS places the payload on an interplanetary transfer to Mars. The JAQAR Astrodynamics Swingby Calculator (SBC) was utilized to calculate the necessary departure C3 values for a range of launch and arrival dates. The departure dates were varied over a 2.1 year span, equal to the synodic period of Mars. To capture the optimal transfer for each launch date and maintain a plausible transfer time, the TOF were varied conservatively between 60 and 600 days. This launch date and TOF sweep was performed with single day steps in each parameter to capture all trajectory possibilities within the defined transfer period. The C3 values were converted to the required ΔV to depart LEO and, with TOF, passed on to the propulsion sizer to define the EDS.

To visualize the optimal launch and arrival date pairings over the entire launch opportunity considered, a contour plot of the departure ΔV across the range of launch and arrival dates was created. Figure 7 shows a pork chop plot, zoomed in on the pair of minimum ΔV opportunities for departure, indicated by the black X's in the figure. A JPL-derived pork-chop plot appears in Figure 8 for comparison and verification of the 2020 opportunity output.

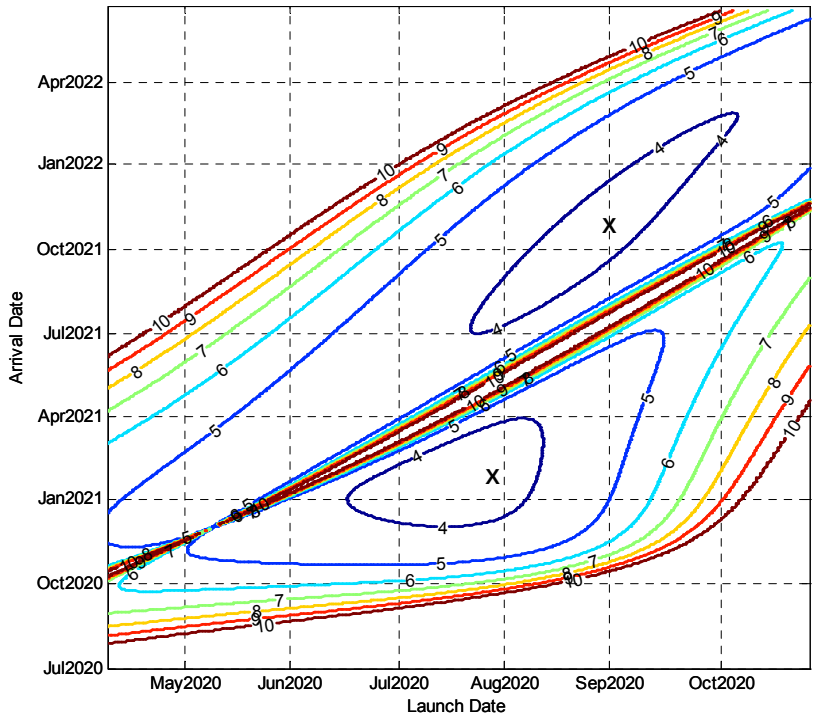

Figure 7. 2020 Earth to Mars Launch Opportunity Pork Chop Plot.

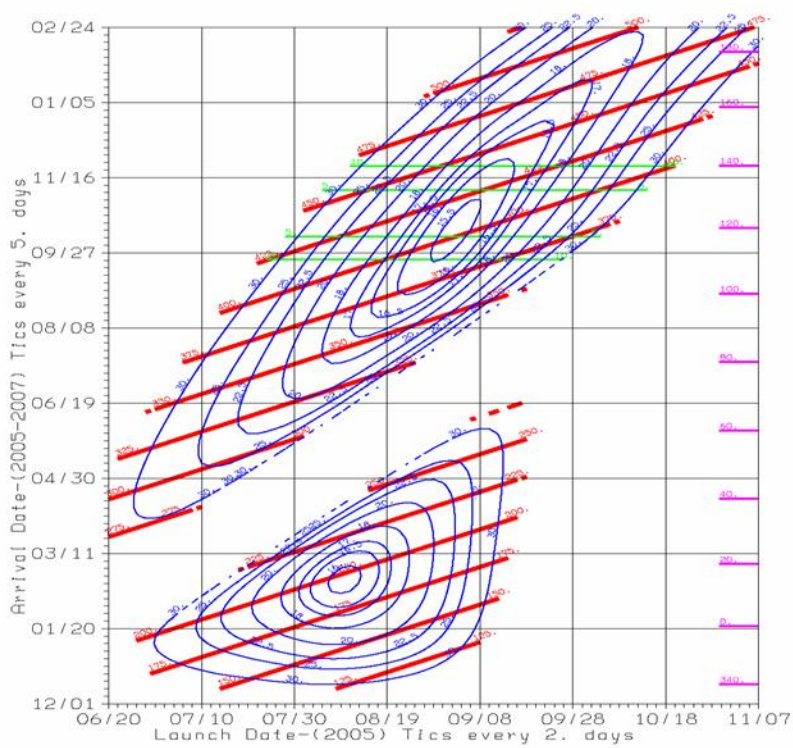

Figure 8. 2005 Earth to Mars Opportunity[9].

The first departure opportunity is a 6-month, type 1 transfer, departing in late July 2020, and the second is a 14-month, type 2 transfer, departing in late August 2020. Figure 9 depicts the minimum ΔV for a given

launch date, as well as the corresponding time of flight for these two opportunities. The minimums are again marked with X's. Because the two opportunities overlap, a 4-month launch window can be defined to span both opportunities, with a maximum TMI ΔV of 4 km/s. This ΔV was baselined as the maximum velocity change that the EDS perform. This ΔV limit affords the design a generous launch window, lasting from June 18 to October 6 in 2020, bounded by the dashed lines in the figure. The two transfers that bound the 2020 launch window and the minimum ΔV type 1 and type 2 transfers appear in Figure 9. The transition from type 1 short-way transfers to type 2 long-way transfers is on August 8, 2020. Departures before this date in the launch window result in transfer times of 6 to 7 months, while departures after this date have flight times from 12 to 17 months. Table 6 summarizes the transfers bounding the launch window and the minimum ΔV transfers.

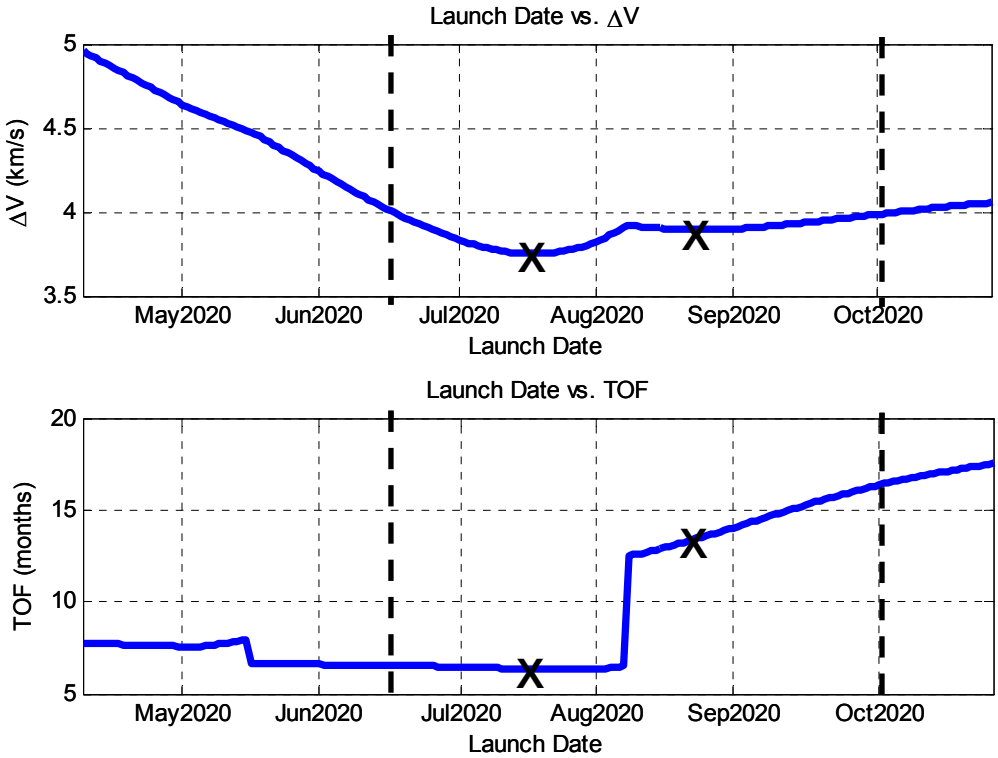

Figure 9. Launch window time of flight and ΔV.

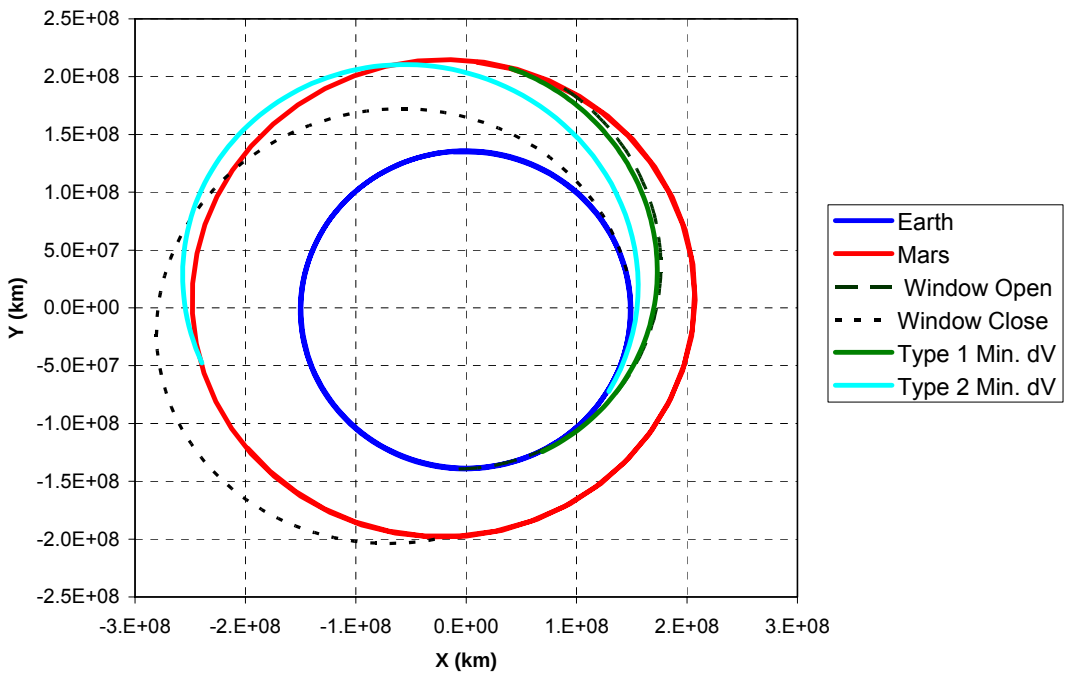

Figure 10. Interplanetary Trajectories for 2020 Launch Window.

Table 6. Interplanetary Transfer Specifications.

Trajectory	*Launch Date*	*Arrival Date*	*TOF (days)*	*TOF (months)*
Open of Launch Window	6/18/2020	1/3/2021	199	7
Type 1 Trajectory Min ΔV	7/19/2020	1/28/2021	193	6
Type 2 Trajectory Min ΔV	8/21/2020	10/1/2021	406	14
Close of Launch Window	10/6/2020	2/23/2022	505	17

Sizing

Propulsion System

Ascent

Propellant mass required for the ascent phase is iteratively developed from the baseline Ares V configuration, payload mass required in LEO, and the optimal ascent trajectory to reach LEO. The propulsion system dry mass for the ascent phase is included in the mass required to LEO.

Transfer

The propulsion system necessary for the transfer phase was sized for a maximum ΔV of 4 km/s to go from LEO to the Mars SOI and associated time of flight for a given launch date within the defined launch window. Based on the FOMs, the propulsion system and propellant type are the strongest drivers for the EDS concept. Accordingly, several heritage propellants and systems currently under development were considered. With the exception of MMH/NTO, all systems were assumed to be pump-fed. The propellants and associated performance parameters are given in Table 7.

Table 7. Propellant Characteristics[2].

	I_{sp} (s)	O/F
MMH/NTO	335	1.64
LOX/LH2	455.2	6
LOX/RP-1	305	2.7
LOX/CH4	350	3.5
LOX/slush LH2	455.2	6
NTR: LH2	950	N/A

	Density (kg/m^3)	Boiloff Rate (kg/day)
MMH	878	0
NTO	1440	0
LOX	1142	8.64
LH2	71	10.8
RP-1	810	0
CH4	423	7.92
slush LH2	330	10.8

Three different types of tanks were traded to assess the impact of storage capability: aluminum, titanium, and titanium overwrapped with carbon fiber. The tanks were sized from propellant pressure MERs for liquid bi-propellant pump-fed engines[2]. To estimate engine dry mass, the engine thrust was approximated as the maximum thrust for an RL-10-class engine (~134 kN) and correlated with mass data on existing bi-propellant engines. The mass of the lines, valves, pumps, and other ancillary components was estimated to be equal to the engine dry mass[3]. Additionally, for the NTR option, the mass of the radiation shield required was included in the propulsion system dry mass estimate.

Line losses, ullage, and boil-off were all accounted for in the propulsion sizing analysis. Line losses were assumed to be on the order of 1.5% for all propellants. Storable propellants assumed a ullage factor of 0.5%, and all other propellants assumed a ullage factor of 2.5%[1,4]. The majority of boil-off losses occur while the vehicle is in LEO, awaiting rendezvous with cargo elements being delivered on separate launches. In addition to accounting for boil-off losses, the boil-off mass was used to assess the potential need for a propellant depot in LEO, should subsequent launches not deliver payloads to LEO within the 14-day window defined by ESAS. The mass of propellant remaining after the TMI burn is limited, and boil-off for this remaining propellant was neglected in this study. Boil-off rates for the cryogenic propellants considered are given in Table 7.

For a given propellant type and tank type, the propulsion sizer iterates on the mass ratio of the EDS until convergence. Final selection of a propulsion system, including propellant and tank types, is not made from the propulsion sizer directly. The outputs of the propulsion sizer are subsequently integrated with power, cost, and reliability to evaluate an entire EDS configuration before a particular system is chosen, as shown in the DSM given in Figure 3.

Other Subsystems

The thermal, attitude determination and control system (ADCS), communications, command and data handling (C&DH) subsystems were not considered to be major drivers in the selection of the EDS architecture. However, to size and trade the full EDS system, it was necessary to accurately size the minor subsystems to be representative of a manned mission to Mars. The power system was also sized but has minimal impact since the selection of a bi-modal NTR eliminated the need for a separate power generator. The sizing rationale for each of these subsystems will be briefly described.

For cases utilizing chemical propulsion and NTR without bi-modal capability, Gallium-Arsenide solar panels were used to power the EDS and payload element. The array mass was estimated from historical power densities and drive masses for articulation. All power systems required a historically-sized power management and distribution system. Additionally, a 300 kW-h of battery capacity was sized for the launch phase.

Analysis of the environment the EDS will experience during the time spent in LEO and also on the interplanetary transfer determined that both passive and active thermal control are required to maintain acceptable equilibrium temperatures. The aft section of the EDS houses the nuclear reactor and requires radiators for heat not captured by the active thermal system or the Brayton engine. The temperature of the EDS and payload element is maintained using variable conductance heat pipes from the reactor. Variable systems were specified because the crewed transfer will require more precise temperature control than the cargo transfers. A nominal pipe length, number of pumps, radiator area, and MLI area were assumed, and component masses were calculated using a mass estimating relation from existing component masses representative of the type considered for this mission.

The ADCS was sized similarly, by first calculating the classes of components required and then using mass estimating relations from appropriate ADCS systems. The sensor suite was derived from previous Mars transfer cruise stages and redundancy was added to all non-redundant systems. Disturbance torques

were estimated to be low in the planetary environment, eliminating the need for complicated control actuators. A system of 24 400 N hydrazine thrusters was selected to perform all attitude adjustments.

The communications and C&DH packages were assumed to be constant, and their masses were defined from current designs for an interplanetary human mission. Since detailed structural design is beyond the scope of this study, a loads analysis was not used to size the structure. Instead, a historical mass estimating relation based on human spacecraft structure was used to estimate the total structural mass for the unpressurized EDS.

Payload Division

Multiple launch solutions were evaluated by varying the fill of the EDS. Varying the fill regimen required remanifesting of payload between different launch vehicles. In the reallocation, the payload was assumed to be divisible in increments, allowing the excess payload to be allocated as mass, neglecting volume considerations. Additionally, if the propellant required for the transfer to Mars exceeded the propellant remaining after ascent to LEO, a propellant depot was added to improve the baseline architecture, allowing for on-orbit refueling of the EDS.

Propellant Depot

The propellant depot was sized using a tool which sizes a complete propellant depot system based on the amount of propellant stored, average fuel storage time, oxidizer-to-fuel ratio, and tank materials These parameters drive the physical size of the tanks and supporting structure, which, in turn, sizes the associated subsystems. This process is iterated upon until the size of the cylindrical tanks meets the size required by the propellant. The depot was assumed to be cylindrical with a docking interface on one end and multiple insulation layers around the tanks. Power is generated by solar panels onboard the depot. The data from this tool was then regressed into a second-order response surface equation as a function of the four primary inputs in order to obtain a parametric relation for the mass of the propellant depot without having to perform the analysis outside of the EDS system loop.

Cost Analysis

A relative cost analysis was performed to evaluate the development and production costs for each alternative. A model based on data obtained from the NASA/Air Force Cost Model (NAFCOM) formed the basis of the cost estimation. NAFCOM uses a historical database of past missions to estimate planned mission cost[6]. To enable a fully parametric analysis, regressed equations for the design, development, test, and evaluation cost, flight unit cost, and production costs were obtained using NAFCOM for the EDS by analogy to the second stage of manned launch vehicles. Similarly, the same cost parameters were obtained for the propellant depot by analogy to unmanned low-Earth orbiting spacecraft. System integration costs were neglected in this analysis as the relative integration complexity variation could not accurately be captured. Most of the elements of the EDS system utilize a second-order response surface equation; however, functions of single variables were regressed about the nominal point using a cubic equation, and the main propulsion dry elements were shown to vary linearly with mass for a given fuel type. An estimated cost for the propellant depot was found as a function of initial on-orbit mass by maintaining constant mass fractions for the all subsystems when regressing the NAFCOM data. The parameters used for each element regression as well as the functional form are shown in Table 8.

Table 8. Cost Estimation Parameters and Functional Form.

Element	*Parameters*	*Functional Form*
Structure and Mechanisms		
Vehicle Structure	Dry Mass, Structural Efficiency	2nd Order RSE
Tank Structure	Dry Mass, Structural Efficiency	2nd Order RSE
Thermal Control	Mass, Type of Thermal Control	2nd Order RSE
Reaction Control	Dry Mass, I_{sp}, Thrust, Propellant Mass	2nd Order RSE
Main Propulsion	Mass (Less Engine), Fuel Type	Linear
Electrical Power/Distribution	Mass, Power Output, Storage Capacity	2nd Order RSE
Command, Control, Data Handling	Mass, Number of Transmitters	2nd Order RSE
Guidance, Navigation, and Control	Mass	Cubic
Engine	Dry Mass, D&D Complexity, D&D Inheritance, Unit Complexity	2nd Order RSE
Propellant Depot	Mass	Power

The following ground rules and assumptions were used in analyzing the cost of the EDS system:

- 8-year development schedule
- 5% fee
- 10% program support for contracted costs
- 30% contingency
- 4% vehicle level integration complexity
- 100% Crawford learning curve
- 3 development units for each subsystem
- 15 unit production run

Additional cost values for the launch were assumed to be $750 million based on estimates for the Ares V[1].

Reliability Analysis

A system reliability analysis was performed by examining the impact of individual component failure rates on the probability of loss of mission (LOM) as well as the probability of loss of vehicle (LOV). LOM is defined as the inability to complete the requirements of the mission, and LOV is the catastrophic loss of the EDS and, if aboard, the crew. In assessing reliability, it was assumed that all events and systems are independent of one another, allowing the probabilities to be expressed for both redundant and serial systems[12]. The subsystem reliabilities associated with the EDS analysis are shown in Table 9.

Table 9. EDS Subsystem Reliabilities.

Subsystem	*Failure Rate (1/Flights)*
Propellant Feed System	1.2×10^{-4}
Avionics and Flight Control	1.5×10^{-5}
Electrical System	8.0×10^{-4}
Attitude Control System	6.7×10^{-4}
Software	1.2×10^{-4}
Propellent Storage System	3.6×10^{-4}
Structure	1.0×10^{-5}
Engines	1.0×10^{-4}
Thermal System	2.0×10^{-4}

Additional factors accounting for propellant type, number of rendezvous performed, and engine out capability were included in the analysis. Additionally, credits were given on LOM for having a propellant depot as the flexibility that the propellant depot provides significant benefits on the probability of mission success. Probabilities for the catastrophic loss of vehicle were accounted for as percentages of the individual failure accountability.

IV. Results

Earth Departure Stage Solutions

Design Space

Figure 11 and Figure 12 show the design space of converged design options normalized with respect to DRM 3.0 values.

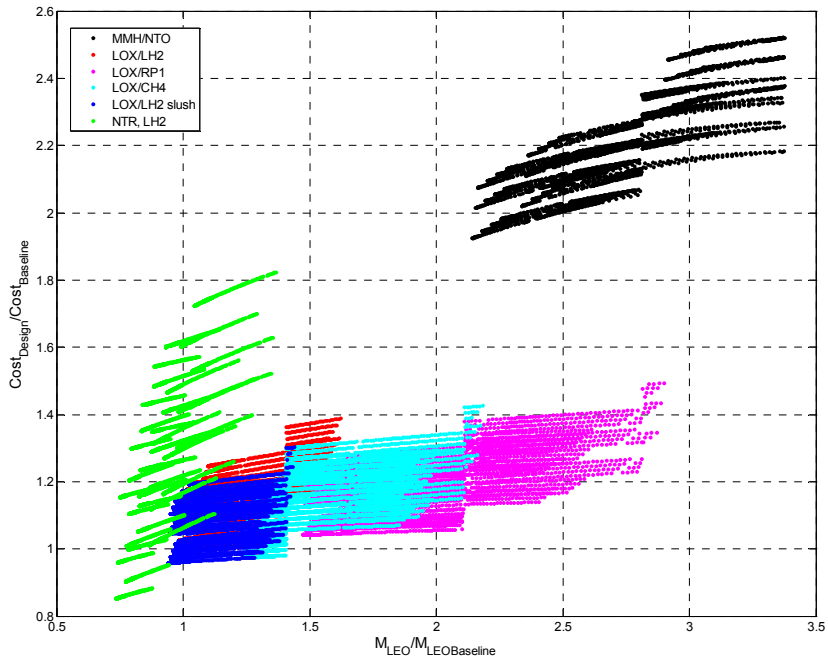

Figure 11. Design Space: Cost Versus LEO Mass.

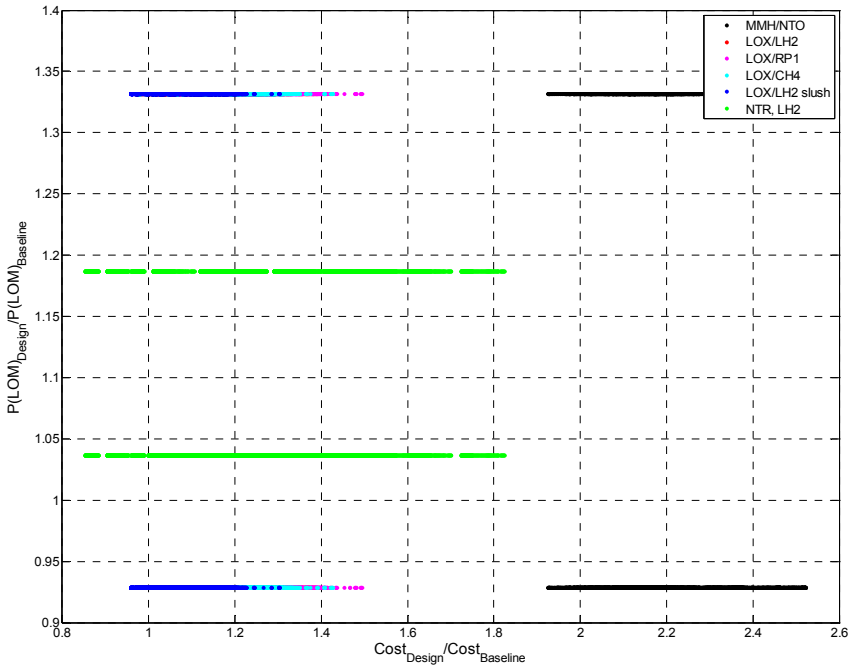

Figure 12. Design Space: Reliability Versus Cost Design Space.

Figure 12 shows two points on the Pareto front exist in the reliability-cost design space investigated. The stratification of the designs is primarily due to the enhancement reliability with engine out capability and a propellant depot in LEO. NTR designs are lower cost solutions than the chemical propulsion systems due to the mass savings associated with the increased specific impulse. The performance increase with NTR over chemical systems is great enough that the boil-off losses for the NTR with LH2 are less than the total

boiloff losses for the chemical bi-propellant systems, which are a function of volume requirements. The LOX/LH2 slush also consistently appears as a viable solution as it has a higher reliability with lower mass associated with the storage of the slush combination. The reliability of all of the chemical systems being of similar order is due to the small contribution the propellant type has on the system reliability.

Factor Contribution to Results

Performing an analysis of variance reveals the percent contribution of each factor to an Overall Evaluation Metric (OEM), calculated for each input combination using the cost and reliability weightings. As shown in Figure 13, engine type and engine-out capability represent 71% and 21% of OEM variability, respectively. Other factors, including ΔV, power type, and tank type, contributed less than 5% to the overall variability of the EDS design.

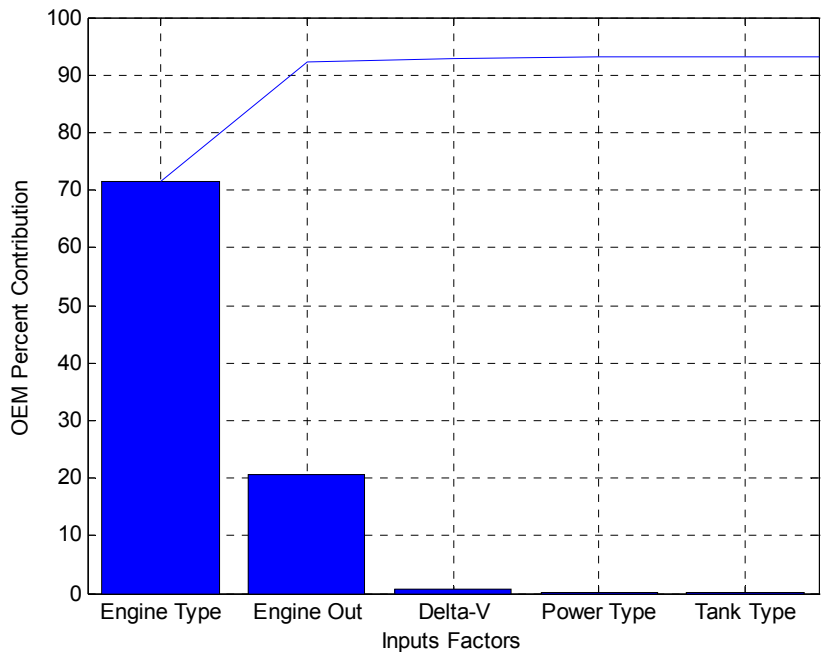

Figure 13. Percent Contribution of Input Factors to OEM.

Selected Design

Vehicle Definition

Depending on the ultimate goal of the design, any design on the Pareto front could be chosen, as all of the designs on the front are non-dominated solutions. TOPSIS was employed to downselect from all of the alternatives to a single EDS design, using a weight for reliability twice as great as cost. A comparison between the selected EDS with the EDS defined by DRM 3.0 is provided in Table 10, with cost, and LOM and LOC normalized by the DRM values obtained through the same analysis process.

Table 10. Selected Design Comparison.

Parameter	*Selected Design*	*Baseline*
Propulsion System	Bi-Modal NTR	NTR
Number of Engines	2	3
Engine Thrust	134 kN	67 kN
Specific Impulse	950 s	~940-960s
Propellant Depot Usage	Yes	No
Propellant Mass Fraction	0.67	0.48
Normalized Cost	0.85	1
Normalized P(LOM)	0.81	1
Normalized P(LOC)	0.81	1

Mass Breakdown

The mass breakdown for the two baseline launches is shown in Table 11. The EDS launch mass is 130.8 MT, and the propellant depot launch mass is 59.5 MT. Approximately 25% of the EDS propellant is launched with the EDS, while the remaining 75% is transferred on orbit from a propellant depot, which was delivered to LEO by a previous launch. By increasing the propellant depot size, a larger payload can supplant the propellant launched with the EDS. Payload capability is also increased by 1,590 kg for cargo missions which do not require a radiation shield.

Table 11. Mass Breakdown for the Vehicle and Propellant Depot Launches.

		Mass (kg)
Interplanetary Stage	Structure	976
	Thermal Control	3,127
	Bi-modal NTR	11,655
	Reactor	*4,215*
	Engines	*1,953*
	PMAD	*342*
	Batteries	*300*
	Shielding	*1,590*
	Coolant & Plumbing	*3,255*
	Comm. and C&DH	320
	GN&C	102
	Reaction Control Subsytem	350
	Tank Mass	3,656
	Dry Mass	**31,841**
	Maximum Payload	74,100
	Propellant	24,859
	Boost Mass	**130,800**
Prop. Depot	Structure and Subsystems	3,694
	PD Propellant	55,806
	PD Boost Mass	**59,500**

Configuration

The configuration of the selected EDS, based on the AHP prioritization vector, is shown below in Figure 14. With payload, the EDS is 56 m long and has a diameter of 8.4 m. The overall configuration is divided into two different segments. One segment contains the NTR propulsion system and associated subsystems along with the LH2 propellant tank. The other segment contains the payload, either manned or unmanned. The two segments are separated by a radiation shield to prevent radiation from the NTR from reaching the crew or cargo. The diameter of the EDS is consistent with the payload fairing of the Ares V to allow for integration into the launch stack.

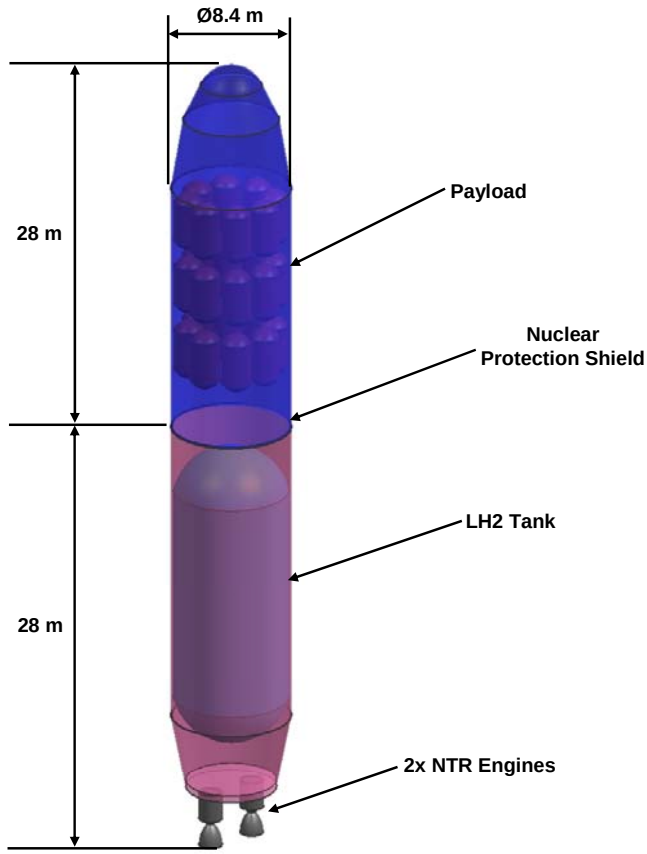

Figure 14. EDS Configuration.

V. Risk Assessment and Mitigation

Risk Assessment

The risks of the development and implementation of this EDS configuration were evaluated and potential mitigation strategies developed. The risks associated with the design of the EDS are detailed in Table 12, along with potential mitigation strategies. Additionally, Figure 15 shows the impact and likelihood of occurrence of each event, with a value of 5 on either axis being the most severe impact or most likely occurrence.

Table 12. Risk Assessment.

ID	*Risk Element*	*Effect*	*Mitigation Strategy*
1	Propulsion System Development	Selected Engine Cannot Be Developed	1. Mission Redesign based on New Engine
2	Failure to Insert in Desired LEO Orbit	Increased Use of Propellant or Loss of Mission	1.Utilize Propellant Reserves 2 .If Ascent Aborted, Loss of Mission
3	Failure to Initiate Appropriate TMI Burn	Increased Use of Propellant or Loss of Mission	1. Utilize Propellant Reserves
4	Engine Failure	Engine Fails to Ignite	1. Single Engine Out Capability
5	Rendezvous Failure	Unable to Fill Propellant Tanks using Propellant Depot	1. Wait for Earth Return Vehicle, Loss of Mission
6	Crew Exposure to Radiation*	Larger Rad Dose than Expected	1. Radiation Shield Thickness Includes Margin 2. High Thrust Transfer Minimizes Exposure to Radiation Belts

*Crewed Missions Only

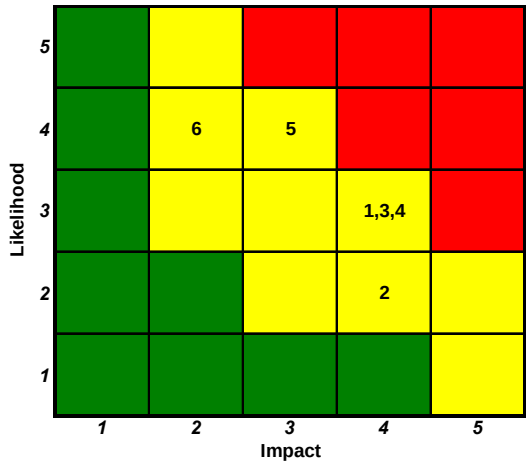

Figure 15. Risk Element Impact and Likelihood of Occurrence.

Technology Impact

Propellant tank mass and insulation can be as much as 15-20% of the propellant mass, a non-negligible factor in sizing the EDS. The three tank types considered in the sizing analysis in this study reaffirmed the case for continuing development of advanced propellant tanks with lower density, higher yield strength, and improved thermal characteristics. With the possibility of having the EDS spend days, or even months, in LEO awaiting launches of additional cargo, the capability of tank materials and insulation to reduce boil-off of the high performance cryogenic propellants is necessary to enable these large missions to Mars.

Additionally, the space environment, specifically thermal cycling and radiation, reduces the effectiveness of materials in providing structural support and insulation as time on orbit increases[14]. Active thermal control systems are likely to be required if on-orbit refueling options are not included in the architecture, increasing the mass of the EDS and not fully eliminating losses due to boil-off. Composite tanks were not traded in this study because of their low TRL for space applications, but the impact of reducing launch mass through less massive propellant storage systems merits the recommendation for continued development of composite structures for propellant tanks.

VI. Conclusions and Further Study

A set of converged EDS design alternatives has been developed through the analysis presented in this study. The Pareto front formed by these designs represent equally good solutions, in which moving to designs not on the front requires degradation with respect to at least one FOM. For the design attributes considered, the EDS configuration was a strong function of the propulsion system type and engine out capability. This study recommends continuing development of NTR for interplanetary transfer propulsion and power, composite tank structures, and propellant depot concepts for refueling in LEO.

A single design on the Pareto front was chosen for comparison to the ESAS/DRM baseline EDS. Weighting reliability twice as much as cost resulted in an EDS design with marginal improvements over the EDS design given in DRM 3.0. The final EDS design evolved from this study is compared against the baseline EDS in Table 13 below.

Table 13. System Comparison.

Parameter	*Selected Design*	*Baseline*
Propulsion System	Bi-Modal NTR	NTR
Number of Engines	2	3
Engine Thrust	134 kN	67 kN
Specific Impulse	950 s	~940-960s
Number of Launches	2	1
Launch Vehicle	Ares V	Ares V
Propellant Depot	Yes	No
Transfer Time	194 Days	224 days
Normalized Reliability	0.81	1
Normalized Cost	0.85	1

References

1. "NASA's Exploration Systems Architecture Study," NASA-TM-2005-214062, Nov. 2005.
2. Humble, R. W., Henry, G. N., Larson, W. J., *Space Propulsion Analysis and Design*, 1st Ed., New York: McGraw-Hill, 1995.
3. Larson, W. J. Wertz, J. R. (Eds.), *Space Mission Analysis and Design*, 3rd Ed., El Segundo: Microcosm Press, 1995.
4. Drake, B. G. (Ed.), "Reference Mission Version 3.0 Addendum to the Human Exploartion of Mars: The Reference Mission of the NASA Mars Exploration Study Team," NASA-SP-6107-ADD, Jun. 1998.
5. Saaty, T. L., *Multicriteria Decision Making: The Analytic Hierachy Process*, Vol. 1., Pittsburgh: RWS Publications, 1990.
6. Young, J., Thompson, R., and Wilhite, A., "Architecture Options for Propellant Resupply of Lunar Exploration Elements," AIAA 2006-7237, *AIAA Space 2006*, San Jose, California, Sep 2006.
7. Kennedy, J., and Eberhart, R., "Particle Swarm Optimization," *Proceedings of the IEEE International Conference on Neural Networks*, Vol. 4, IEEE, Perth, WA, Australia, 1995, pp.1942-1948.
8. Grant, M. and Mendeck. G., "Mars Science Laboratory Entry Optimization Using Particle Swarm Methodology," (accepted for publication at AIAA Atmospheric Flight Mechanics Conference and Exhibit 2007).
9. *Jet Propulsion Laboratory Mars Exploration: Features*, 22 Mar. 2006. Jet Propulsion Laboratory. 20 Feb. 2007 <http://marsprogram.jpl.nasa.gov/spotlight/porkchop-image01.html>.
10. Smith, K. Winn, S. et. al., "NAFCOM Cost Model," Science Applications International Corporation, Jun. 2004.
11. "NASA's Exploration Systems Architecture Study," NASA-TM-2005-214062, Nov. 2005.
12. Larson. W. J., Pranke, L. K., *Human Spaceflight: Mission Analysis and Design*, 1st Ed., New York: McGraw Hill, 1999.
13. Powell, R. W., Striepe, S. A., Desai, P. N., and Braun, R. D., "Program to Optimize Simulated Trajectories (POST) Utilization Manual," Martin Marietta Corporation, Vol. II, Version 5.2, Oct. 1997.
14. Tribble, A. C., *The Space Environment: Implications for Spacecraft Design*, Princeton: Princeton University Press, 1995.